Electronic Supplementary Material (ESI) for Dalton Transactions.

Supplementary Materials

Constructing Spin Crossover-Fluorescence Bifunctional Iron(II) complexes based on Tetraphenyl Ethylene-Decorated AIEgen

Cheng Yi [a], Shi-Hui Zhang,[a] Liang Zhao [a], Nian-Tao Yao [a], Guo-Hui Zhao, Yin-Shan Meng [a], Tao Liu [a] *

[a]*State Key Laboratory of Fine Chemicals, Dalian University of Technology, Dalian, 116024, P. R. China*

E-mail: liutao@dlut.edu.cn (T. Liu)

CONTENTS

Experimental section.

Materials

Tpe-CHO, bpp-COOH, bpp-COOEt, bpp-CH_2OH, bpp-CH_2Br, and bpp-$CH_2P(O)(OEt)_2$ were prepared according to literature methods[1]. All other chemicals are commercially available and were used without further purification.

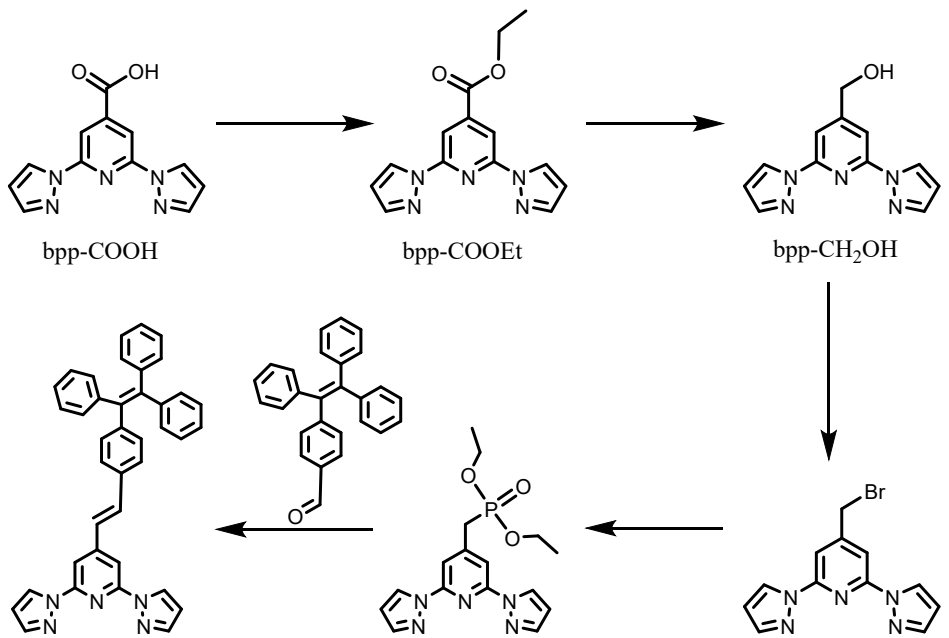

Scheme S1

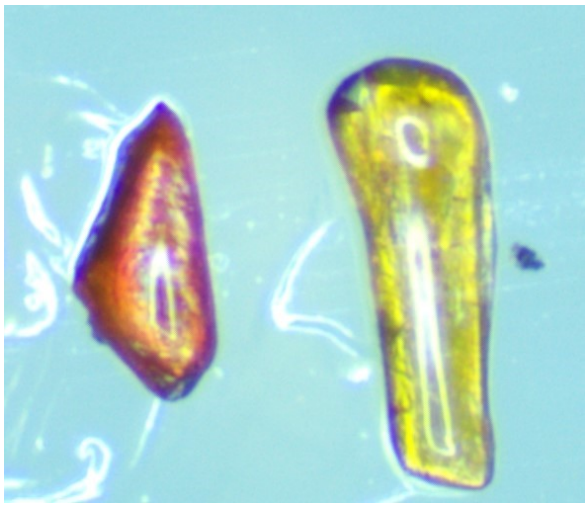

Fig. S1. Photographs of single crystals for **1** and **2** in the vacuum grease under the optical microscope at room temperature.

Table S1. Crystallographic data for **1**, **2**, and **3** at different temperatures.

Compounds	**1**	**2**	**2**	**3**	**3**
CCDC	2226385	2225794	2225800	2225801	2225804
T, K	120	120	275K	120	275
*F*w	1634.25	1551.10	1551.10	1516.48	1517.11
crystal system	Triclinic	Triclinic	Triclinic	Triclinic	Triclinic
Space group	$P\bar{1}$	$P\bar{1}$	$P\bar{1}$	$P\bar{1}$	$P\bar{1}$
a, Å	14.5133(19)	12.9914(6)	13.207(3)	12.8968(7)	13.064(4)
b, Å	23.240(4)	17.0329(8)	17.273(3)	16.9841(9)	17.158(6)
c, Å	24.914(4)	18.9494(8)	19.209(3)	19.0169(11)	19.208(6)
α, °	105.490(6)	63.7760(10)	63.904(5)	63.584(2)	63.673(10)
β, °	101.434(6)	84.270(2)	84.196(6)	83.769(2)	84.103(12)
γ, °	101.383(5)	86.755(2)	86.212(7)	86.568(2)	86.368(12)
V, Å^3	7654(2)	3742.4(3)	3914.0(12	3708.2(4)	3838(2)
Z	4	2	2	2	2
D_{calc} (mg/m^3)	1418	1376	1314	1358	1313
F (000)	3363.0	1612.0	1610.0	1571.0	1572.0
Reflections collected	146531	40737	57443	28903	34320
Unique reflections (R_{int})	34866(0.0373)	13655(0.0566)	14309(0.0661)	13075(0.0582)	13257(0.0595)
Goodness–of–fit on F^2	1.038	1.027	1.031	1.048	1.026
R_1 [$I>2\sigma(I)$][a]	0.0567	0.0524	0.0620	0.0664	0.0652
wR_2[$I>2\sigma(I)$][b]	0.1439	0.1288	0.1611	0.1700	0.1729

$R_1 = \Sigma\,(|F_o|-|F_c|) / \Sigma\,|F_o|$; $wR_2 = [\Sigma\, w\,(|F_o|-|F_c|)^2 / \Sigma\, w\, F_o^2]^{1/2}$

Table S2. Selected Bond lengths (Å) for **1, 2** and **3** at different temperatures.

1				**2**			**3**	
120 K					120 K	275 K	120 K	275 K
No	Length(Å)	No	Length(Å)	No	Length(Å)	Length(Å)	Length(Å)	Length(Å)
Fe1–N1	1.896(1)	Fe2–N11	1.896(1)	Fe1–N1	1.906(2)	2.113(3)	1.900(4)	2.106(3)
Fe1–N2	1.984(2)	Fe2–N12	1.976(2)	Fe1–N2	1.980(3)	2.191(4)	1.975(5)	2.178(4)
Fe1–N3	1.976(1)	Fe2–N13	1.976(2)	Fe1–N3	1.972(2)	2.171(3)	1.978(5)	2.168(4)
Fe1–N4	1.897(1)	Fe2–N14	1.897(1)	Fe1–N4	1.905(2)	2.132(3)	1.897(5)	2.124(4)
Fe1–N5	1.964(1)	Fe2–N15	1.976(2)	Fe1–N5	1.996(2)	2.202(4)	1.992(5)	2.193(5)
Fe1–N6	1.977(1)	Fe2–N16	1.983(2)	Fe1–N6	1.987(2)	2.192(3)	1.984(5)	2.185(4)
Fe1–N_{avg}	1.949	Fe2–N_{avg}	1.951	Fe1–N_{avg}	1.958	2.167	1.959	2.159

Table S3. Selected Bond Angles (º) for **1** at 120 K.

		1	
N2–Fe1–N6	92.50(8)	N13–Fe2–N12	160.00(8)
N2–Fe1–N5	92.22(8)	N13–Fe2–N15	91.28(9)
N4–Fe1–N2	99.56(8)	N14–Fe2–N13	100.07(8)
N4–Fe1–N1	178.32(8)	N14–Fe2–N16	79.84(8)
N4–Fe1–N3	100.60(8)	N14–Fe2–N12	99.90(8)
N4–Fe1–N6	79.88(8)	N14–Fe2–N15	80.33(8)
N4–Fe1–N5	80.18(8)	N16–Fe2–N13	92.20(8)
N1–Fe1–N2	79.88(8)	N16–Fe2–N12	92.34(8)
N1–Fe1–N3	80.02(8)	N16–Fe2–N15	160.17(8)
N1–Fe1–N6	98.54(8)	N11–Fe2–N13	80.19(8)
N1–Fe1–N5	101.41(8)	N11–Fe2–N14	179.67(8)
N3–Fe1–N2	159.76(8)	N11–Fe2–N16	99.95(8)
N3–Fe1–N6	92.79(8)	N11–Fe2–N12	79.84(8)
N3–Fe1–N5	89.44(8)	N11–Fe2–N15	99.89(8)
N5–Fe1–N6	160.01(7)	N15–Fe2–N12	91.02(8)
Σ_{Fe1}	88.22	Σ_{Fe2}	86.45
$CShM_{Fe1}$	2.117	$CShM_{Fe2}$	2.064

Σ_{Fe} : the sum of | 90-α |for the 12 cis-N-Fe-N angles around the iron atom. $CShM_{Fe}$: the continuous shape measurement relative to ideal octahedron of the Fe center.

Table S4. Selected Bond Angles (º) for **2** and **3** at different temperatures.

Compound	**2**	**2**	**3**	**3**
Temperature(K)	120	275	120	275
N2–Fe1–N6	93.50(10)	95.20(11)	93.53(13)	95.25(12)
N2–Fe1–N5	90.82(10)	94.39(12)	90.88(13)	94.13(12)
N4–Fe1–N2	100.70(9)	107.14(10)	100.41(13)	107.03(11)
N4–Fe1–N1	179.21(10)	177.37(10)	179.37(14)	178.44(11)
N4–Fe1–N3	100.06(10)	105.42(10)	100.09(13)	105.43(11)
N4–Fe1–N6	79.94(9)	73.59(10)	79.85(13)	73.63(11)
N4–Fe1–N5	79.35(9)	73.08(10)	79.55(14)	73.16(11)
N1–Fe1–N2	79.54(9)	73.47(10)	79.64(13)	73.66(10)
N1–Fe1–N3	79.71(9)	74.06(10)	79.88(13)	73.94(10)
N1–Fe1–N6	100.81(9)	108.97(10)	100.78(13)	107.76(11)
N1–Fe1–N5	99.90(9)	104.36(10)	99.83(13)	105.45(11)
N3–Fe1–N2	159.22(9)	147.41(9)	159.49(13)	147.48(10)
N3–Fe1–N6	89.42(9)	92.69(11)	89.15(13)	92.00(12)
N3–Fe1–N5	93.69(10)	96.17(12)	93.74(14)	96.95(12)
N5–Fe1–N6	159.28(9)	146.67(10)	159.38(13)	146.79(11)
Σ_{Fe1}	91.52	150.14	91.19	149.61
$CShM_{Fe1}$	2.249	5.500	2.215	5.464

Σ_{Fe} : the sum of | 90-α |for the 12 cis-N-Fe-N angles around the iron atom. $CShM_{Fe}$: the continuous shape measurement relative to the ideal octahedron of the Fe center.

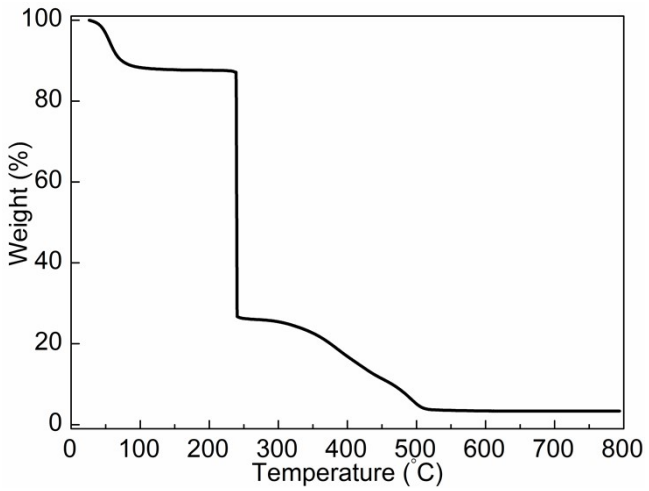

Fig. S2 TGA curve for complex **1** in N_2 atmosphere with a heating rate of 10 ℃·min^{-1}.

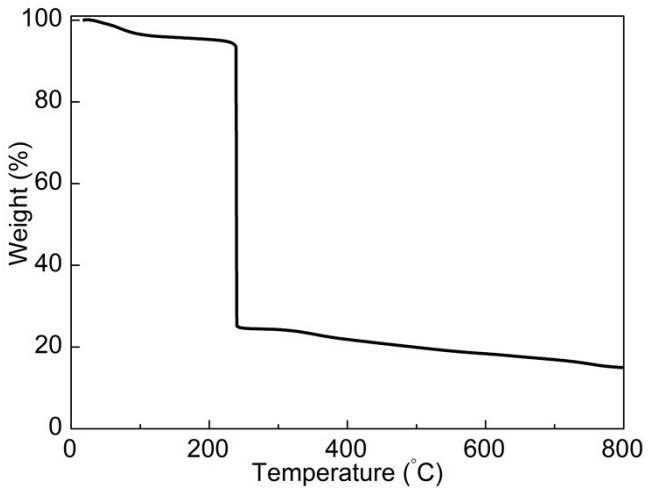

Fig. S3 TGA curve for complex **2** in N_2 atmosphere with a heating rate of 10 ℃·min^{-1}.

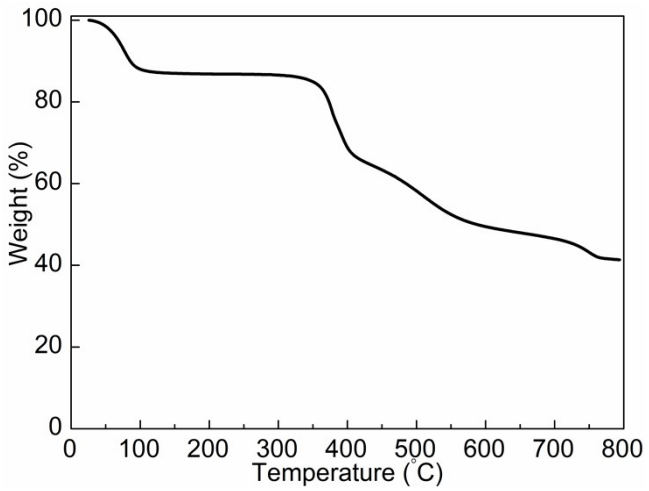

Fig. S4 TGA curve for complex **3** in N_2 atmosphere with a heating rate of 10 ℃·min^{-1}.

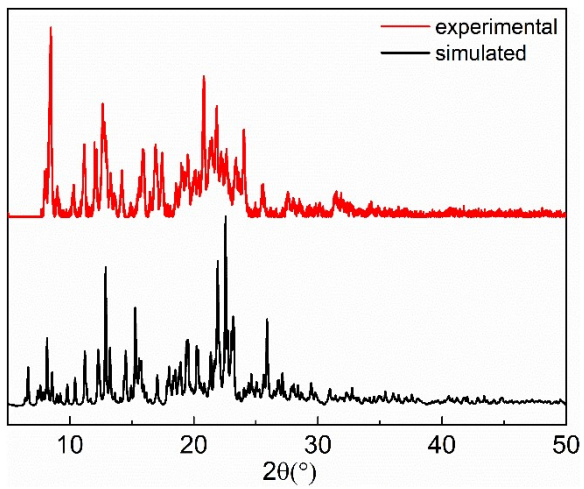

Fig. S5 The PXRD pattern of complex **1** and the simulated one based on the single-crystal structure.

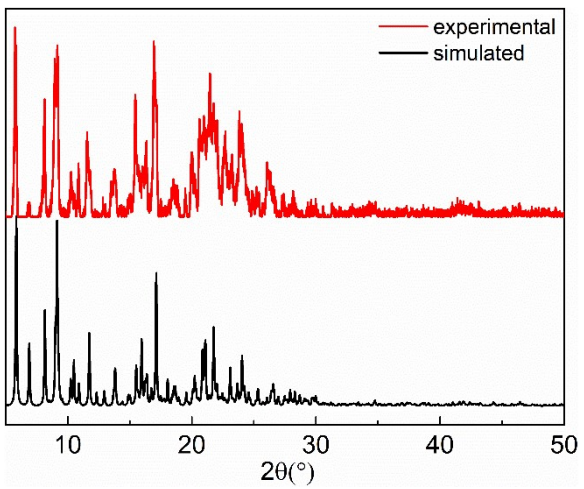

Fig. S6 The PXRD pattern of complex **2** and the simulated one based on the single-crystal structure.

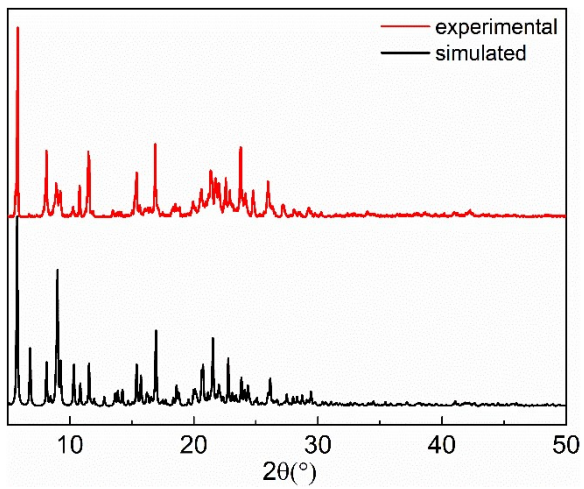

Fig. S7 The PXRD pattern of complex **3** and the simulated one based on the single-crystal structure.

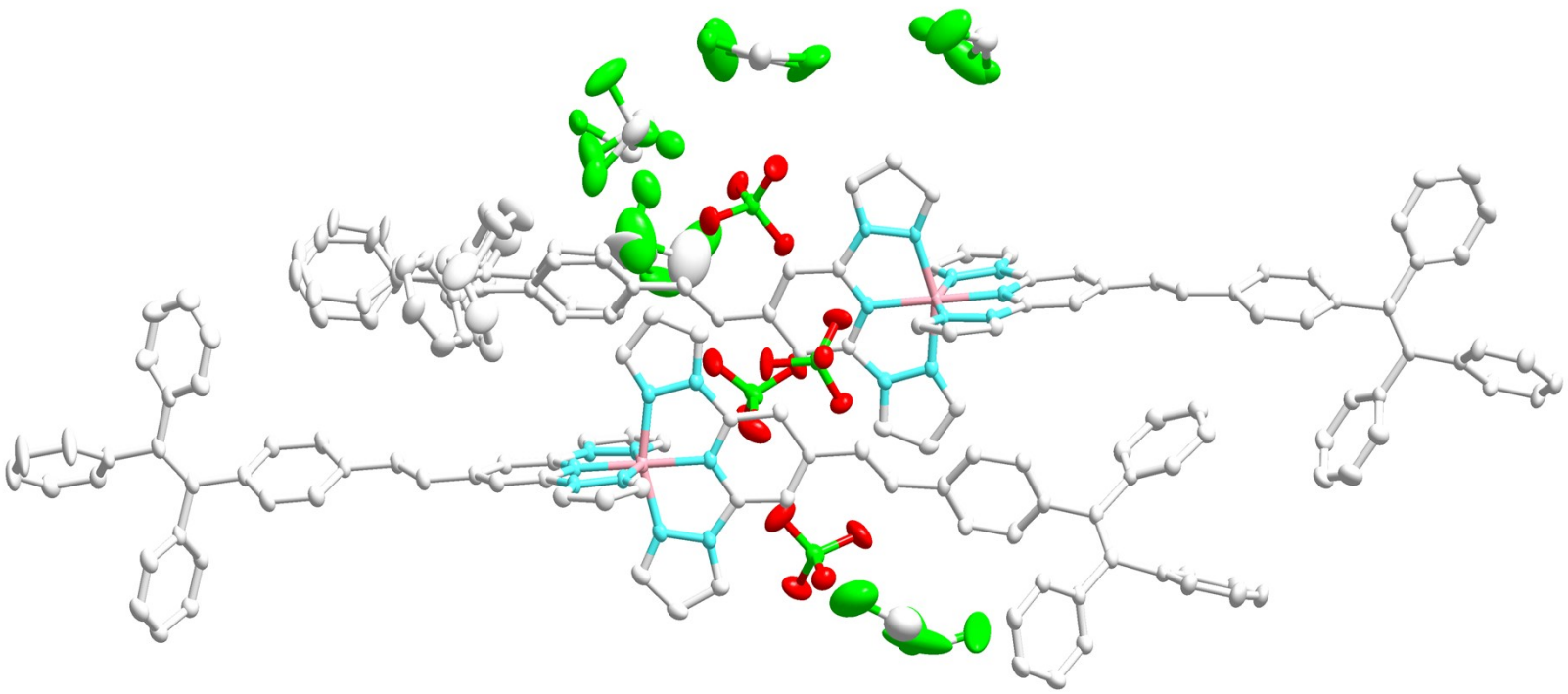

Fig. S8 The Crystal structure of **1** at 120 K.

Top

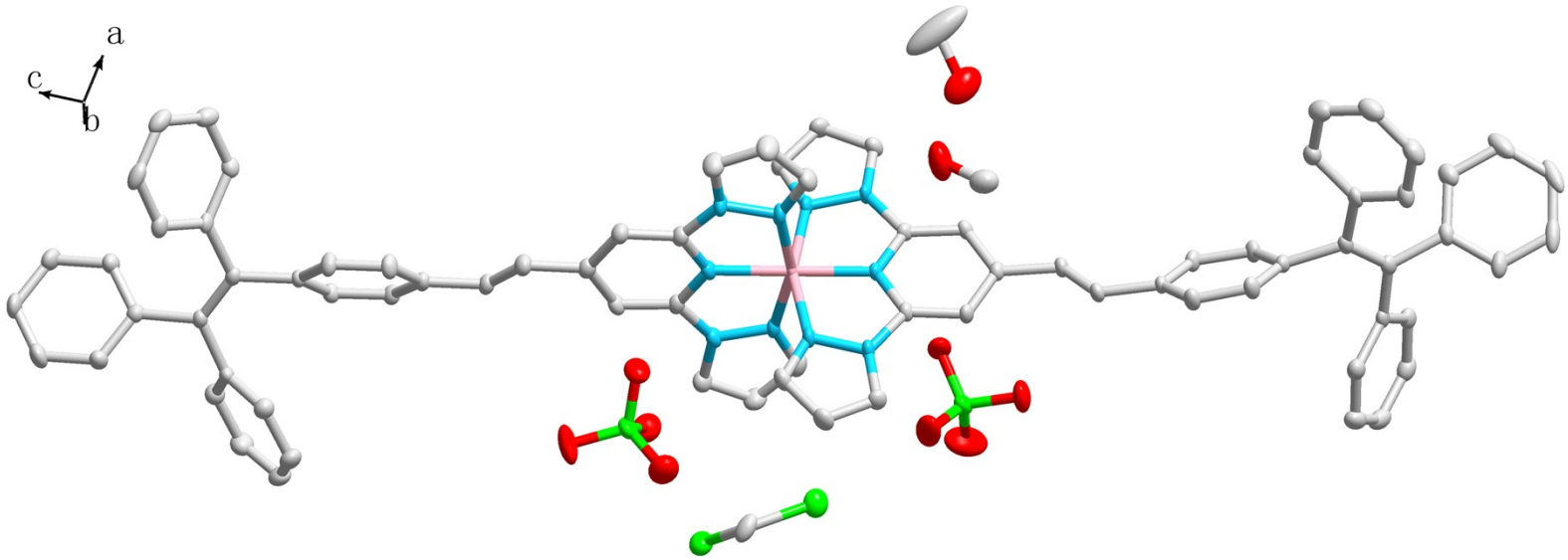

Bottom

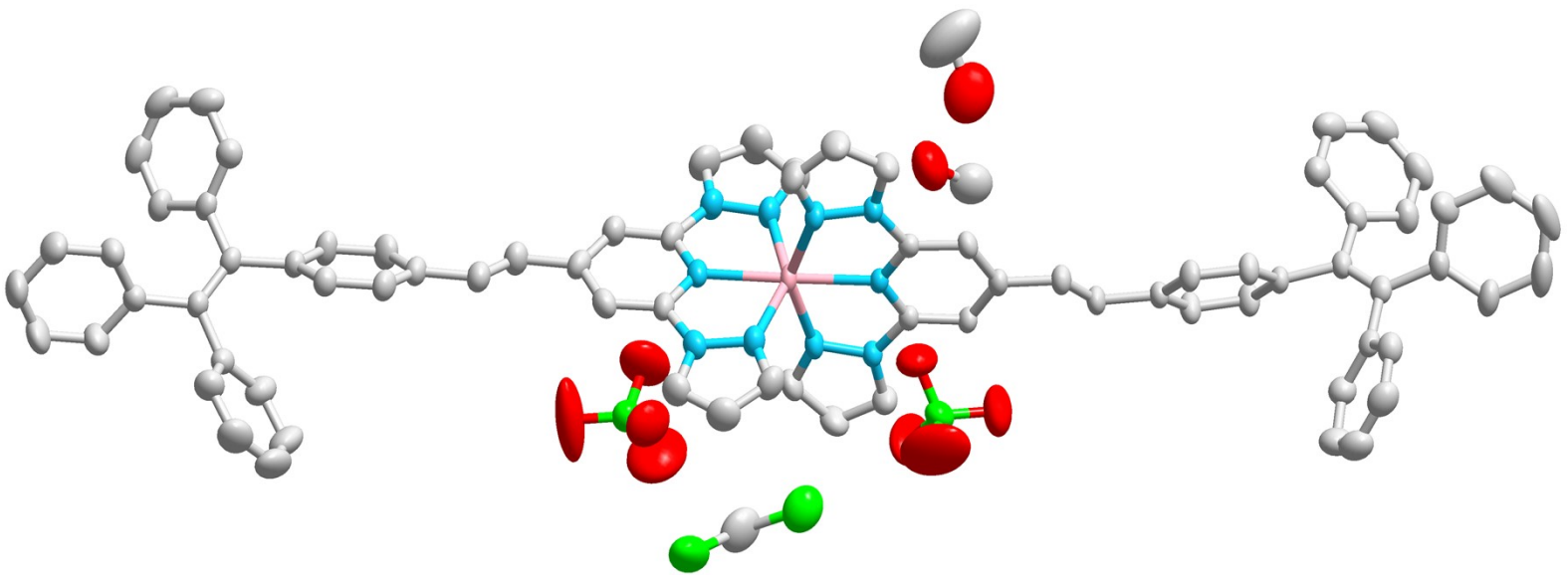

Fig. S9 The Crystal structure of **2** at 120 (top) and 275 (bottom) K.

Top

Bottom

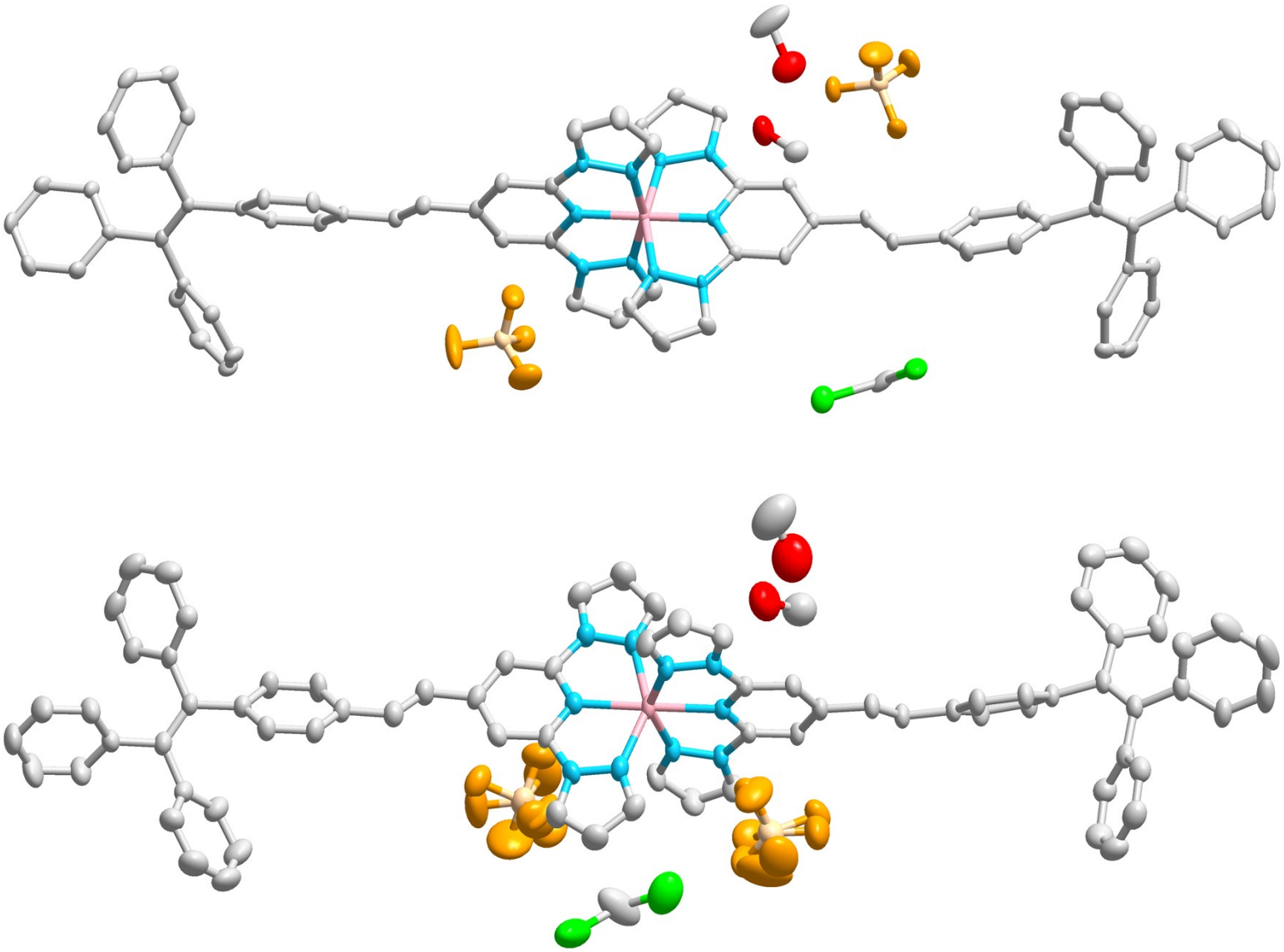

Fig. S10 The Crystal structure of **3** at 120 (top) and 275 (bottom) K.

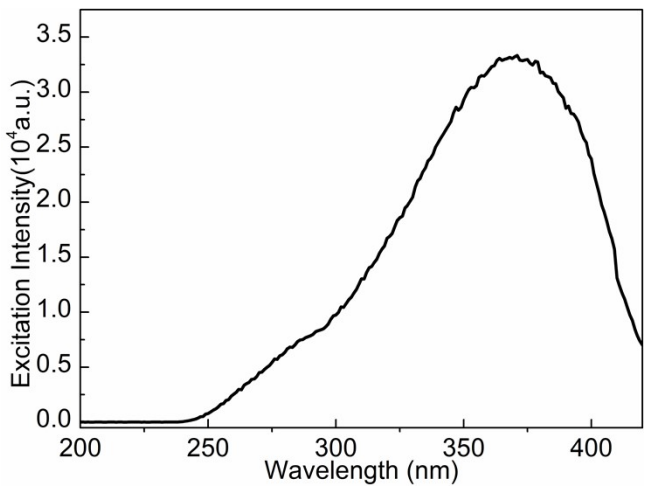

Fig. S11 Fluorescence excitation spectra for the ligand tpe-bpp in pure DMF solution.

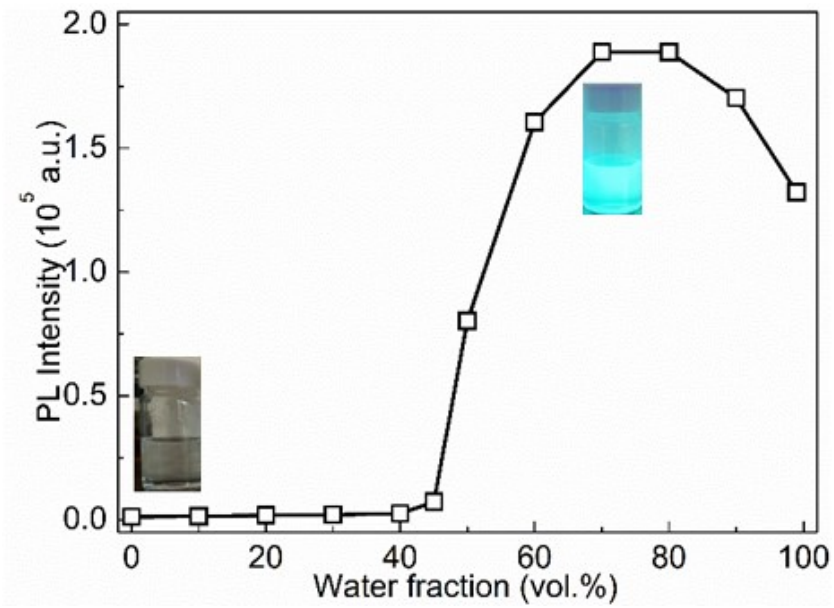

Fig. S12. PL intensity at maximum PL intensity as a function of water fraction for tpe-bpp at room temperature. Inset showed the photographs of tpe-bpp in DMF/water mixtures with different water fractions under 365 nm UV illumination.

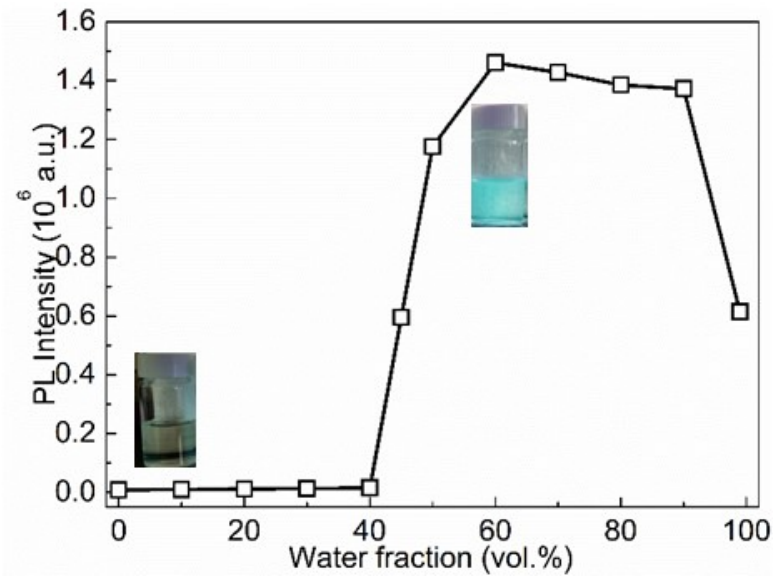

Fig. S13. PL intensity at maximum PL intensity as a function of water fraction for **1** at room temperature. Inset showed the photographs of **1** in DMF/water mixtures with different water fractions under 365 nm UV illumination.

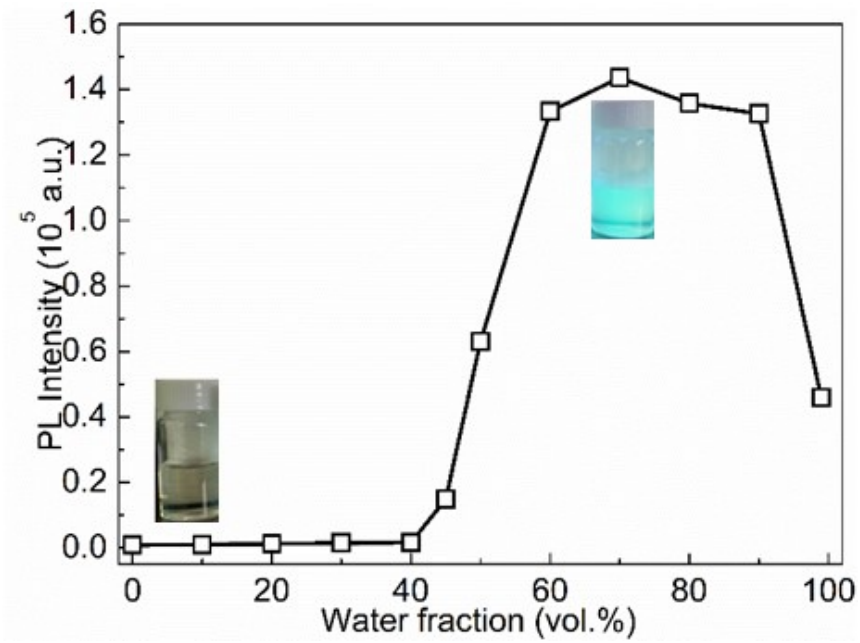

Fig. S14. PL intensity at maximum PL intensity as a function of water fraction for **3** at room temperature. Inset showed the photographs of **3** in DMF/water mixtures with different water fractions under 365 nm UV illumination.

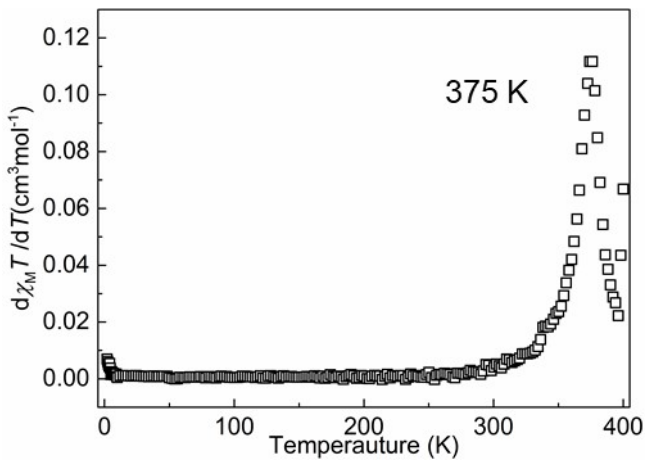

Fig. S15. d($\chi_M T$)/dT versus T for complex **1**.

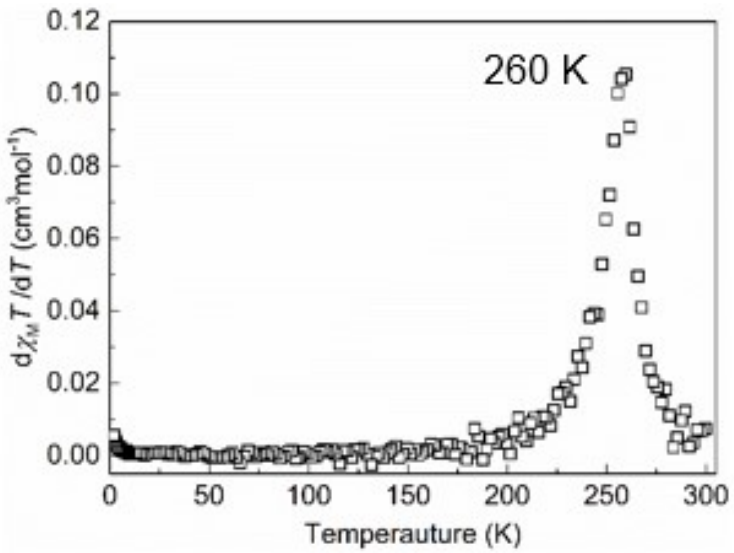

Fig. S16. d($\chi_M T$)/dT versus T for complex **2**.

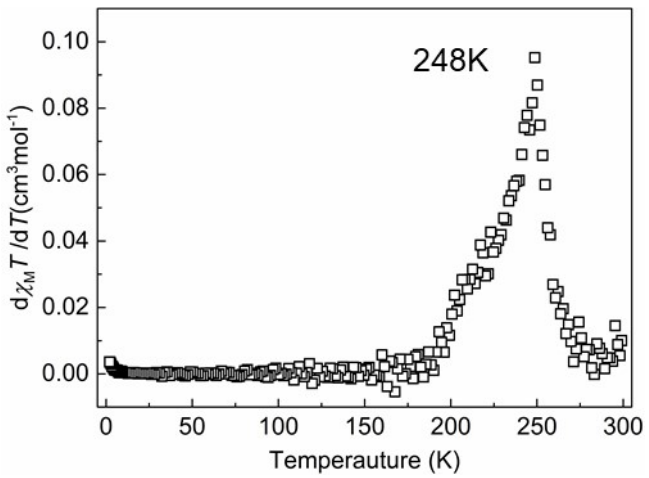

Fig. S17. d($\chi_M T$)/dT versus T for complex **3**.

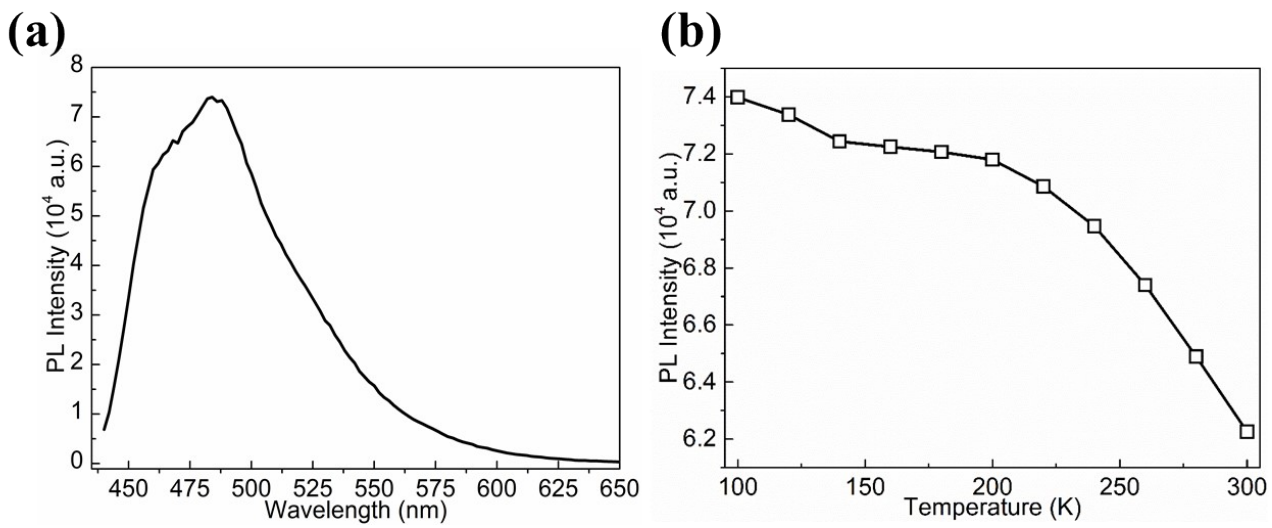

Fig. S18 (a) Luminescence emission spectrum for the tpe-bpp ligand in the solid state at 100 K. (b) The PL intensity of maximum emission as a function of temperature for solid tpe-bpp.

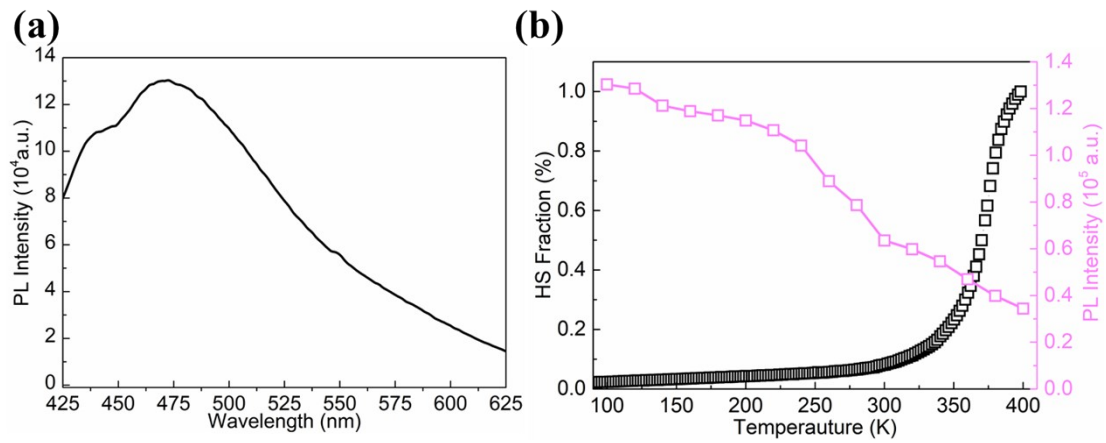

Fig. S19 Luminescence emission spectrum for the complex **1** in solid state at 100 K. (b) Plots of the HS fraction of Fe^{II} ion (□ black squares) and the PL intensity of maximum emission (□ pink squares) as a function of temperature for solid **1**.

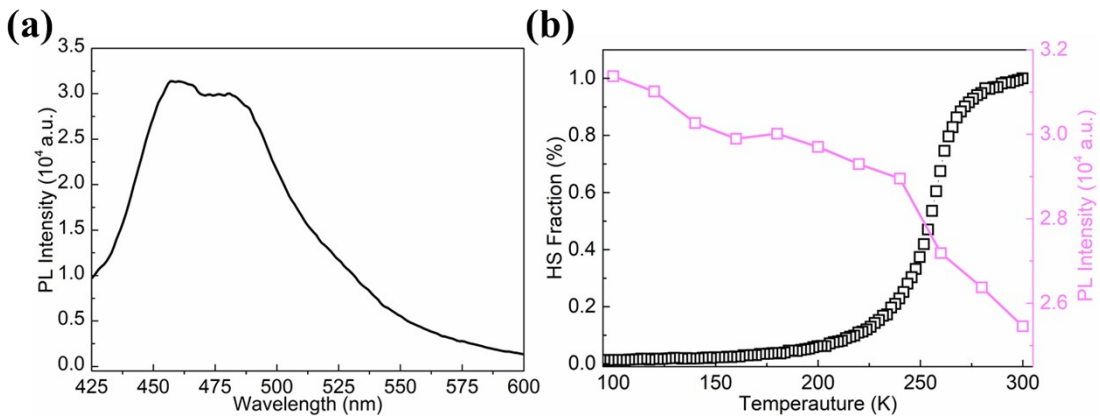

Fig. S20 Luminescence emission spectrum for the complex **2** in solid state at 100 K. (b) Plots of the HS fraction of Fe^{II} ion (□ black squares) and the PL intensity of maximum emission (□ pink squares) as a function of temperature for solid **2**.

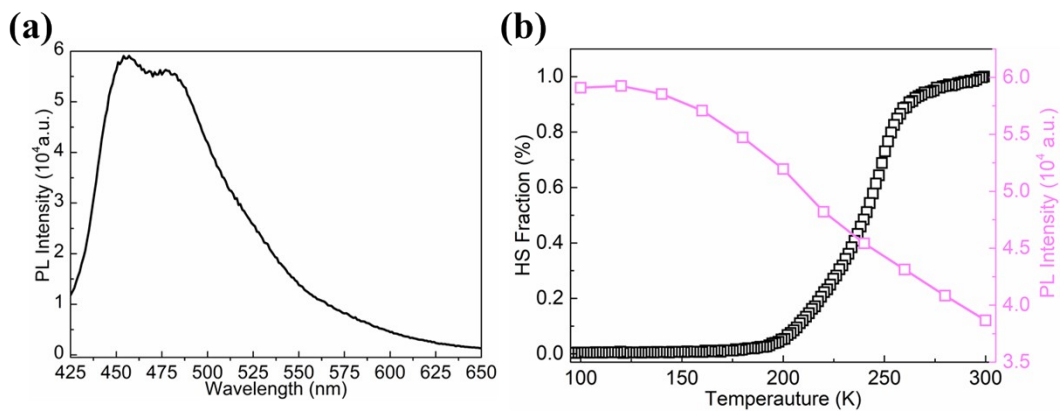

Fig. S21 Luminescence emission spectrum for the complex **3** in solid state at 100 K. (b) Plots of the HS fraction of Fe^{II} ion (□ black squares) and the PL intensity of maximum emission (□ pink squares) as a function of temperature for solid **3**.

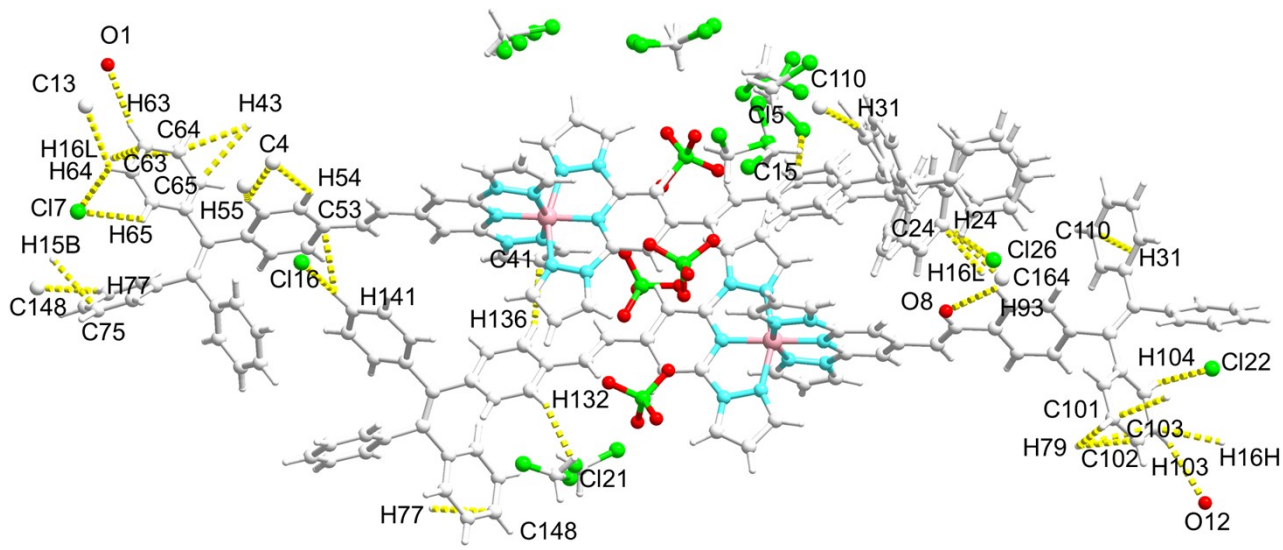

Fig. S22 The intermolecular short contact interactions between tpe units and other groups for **1** at 120 K (yellow dashed lines).

Top

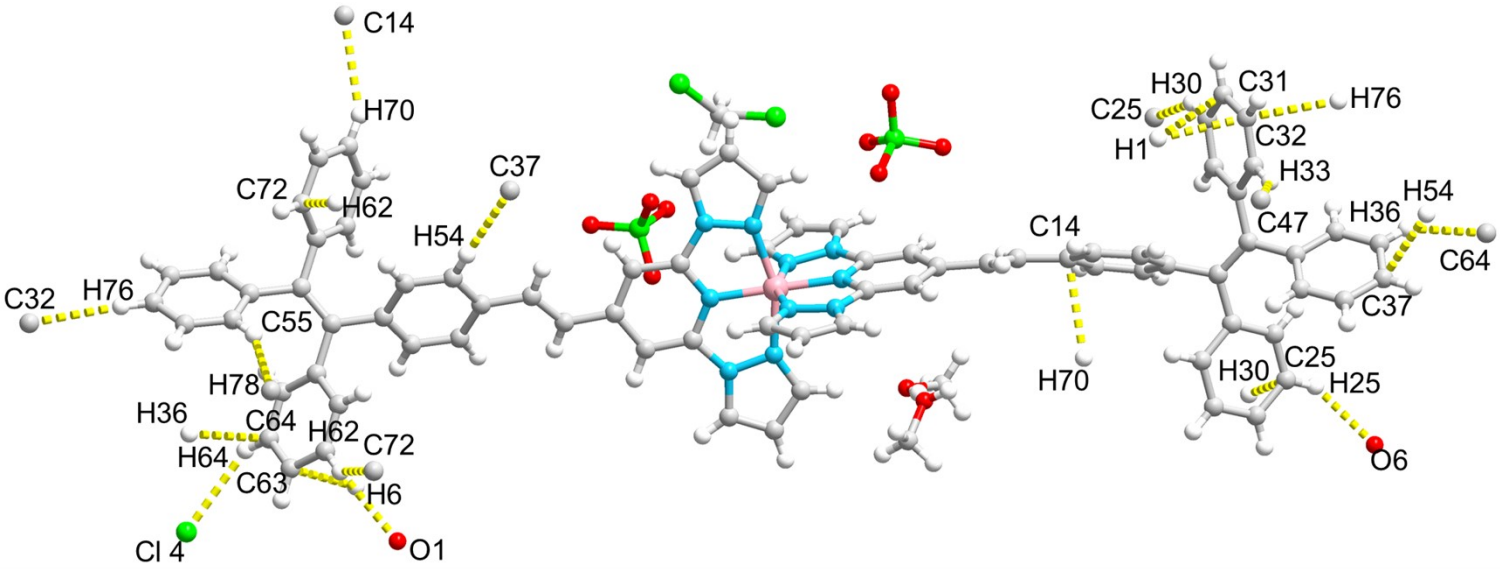

Bottom

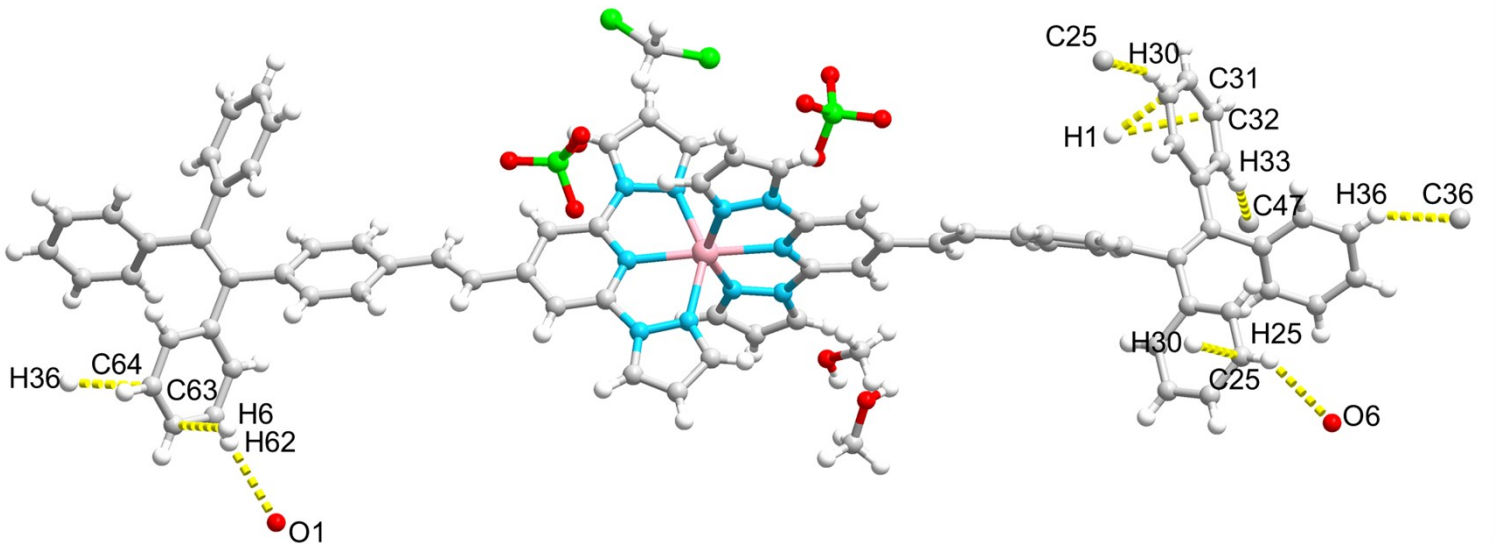

Fig. S23 The intermolecular short contact interactions (yellow dashed lines) between tpe units and other groups for **2** at 120K (top) and 275 K (bottom).

Top

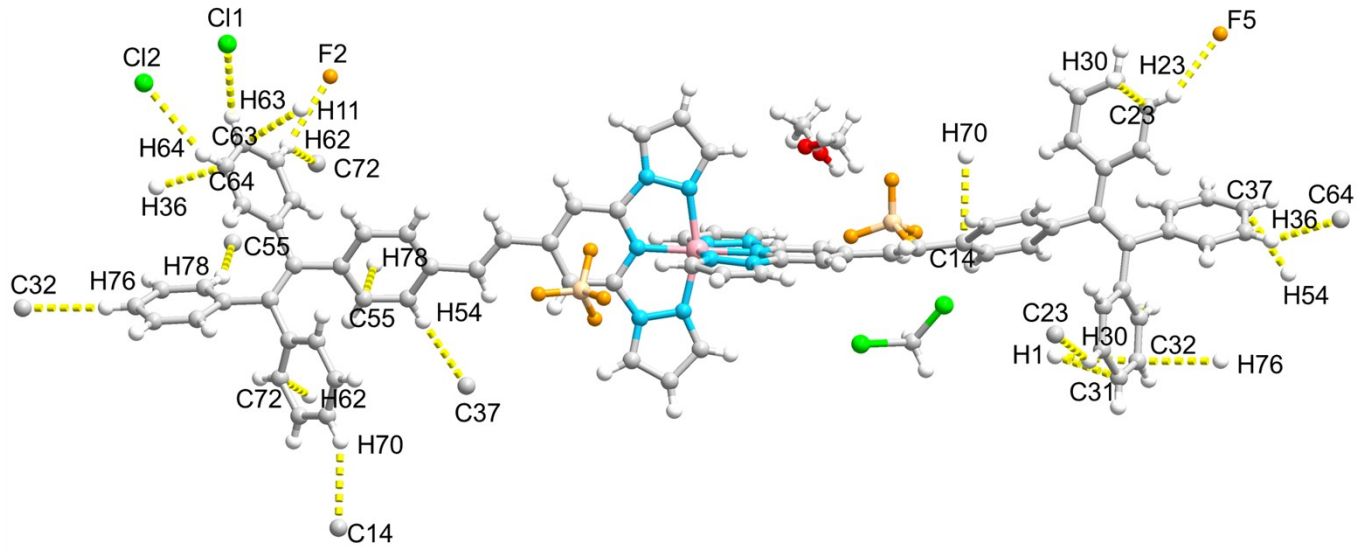

Bottom

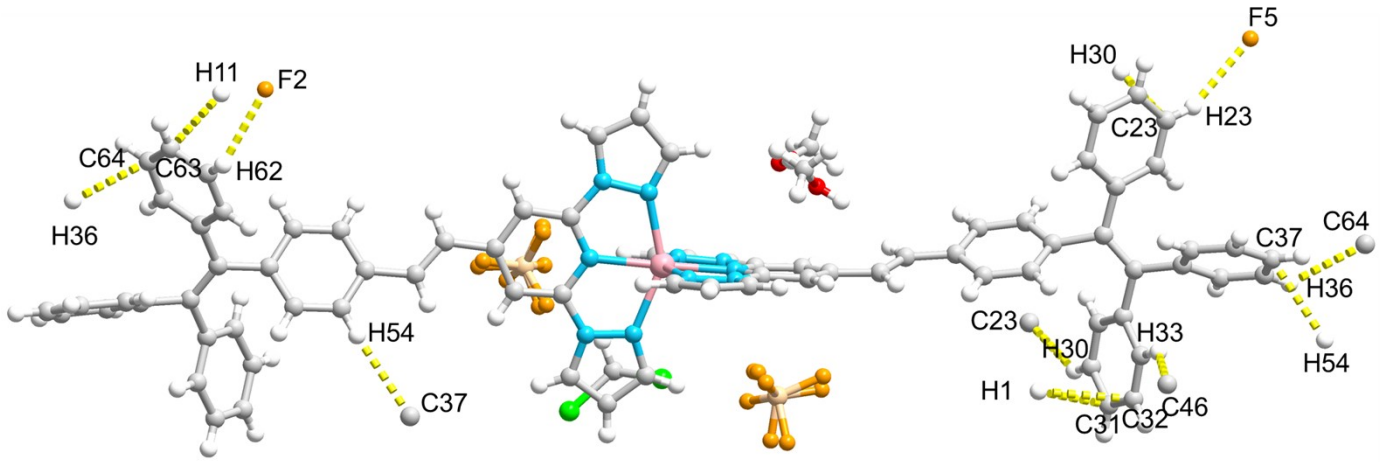

Fig. S24 The intermolecular short contact interactions (yellow dashed lines) between tpe units and other groups for **3** at 120 (top) and 300 (bottom) K.

Table S5. Short contact interactions between phenyl and other groups for **1** at 120 K.

1			
C15 – H15···Cl 9	2.642	C65 – H65···Cl 7	2.856
C24 – H24···Cl 23	2.440	C75···H15B – C158	2.583
C24 – H24···C164	2.497	C77 – H77···C148	2.880
C24···H16L – C164	2.603	C93 – H93···O8	2.625
C25 – H25···Cl 23	2.904	C101···H79 – C79	2.851

C31 – H31···C110	2.676	C101···H142– C142	2.828
C53···H141 – C141	2.877	C102···H79 – C79	2.731
C54 – H54···C4	2.811	C103···H79 – C79	2.855
C55 – H55···C4	2.842	C103 – H103···O12	2.699
C55 – H55···C5	2.792	C103···H16H – C161	2.718
C55 – H55···C6	2.822	C104 – H104···Cl 22	2.853
C61···H49 – C43	2.838	C110···H31 – C31	2.676
C62···H49 – C43	2.869	C132 – H132···Cl 21	2.611
C62···H16L – C164	2.898	C132···H16O – C163	2.817
C63···H16L – C164	2.537	C136 – H136···C41	2.814
C63 – H63···O1	2.563	C141 – H141···C53	2.877
C64 – H64···C13	2.828	C141 – H141···Cl 6	2.944
C64 – H64···Cl 7	2.861	C148···H77 – C77	2.880

Table S6. Short contact interactions between phenyl and other groups for **2** at 120 and 275 K.

2			
120 K		275 K	
C14···H70 – C70	2.886		
C25 – H25···O6	2.436	C25 – H25···O6	2.653
C25···H30 – C30	2.834	C25···H30 – C30	2.861
C30 – H30···C25	2.834	C30 – H30···C25	2.861
C31···H1 – C1	2.714	C31···H1 – C1	2.755
C32···H1 – C1	2.657	C32···H1 – C1	2.813
C32···H76 – C76	2.870		
C33 – H33···C47	2.820	C33 – H33···C47	2.879
C36 – H36···C64	2.697	C36 – H36···C64	2.805
C37···H54 – C54	2.755	C62 – H62···O1	2.691
C54 – H54···C37	2.755	C63···H6– C6	2.806
C55···H78– C78	2.852	C64···H36– C36	2.805
C62 – H62···C72	2.825		
C62 – H62···O1	2.611		
C63···H6– C6	2.762		
C64 – H64···Cl 4	2.924		
C64···H36– C36	2.697		
C70 – H70···Cl4	2.886		
C72···H62– C62	2.825		
C76 – H76···C32	2.870		
C78 – H78···C55	2.852		

Table S7. Short contact interactions between phenyl and other groups for **3** at 120 and 275 K.

3			
120 K		275 K	
C14···H70 – C70	2.847		
C23···H30 – C30	2.850	C23···H30 – C30	2.850
C23 – H23···F5	2.450	C23 – H23···F5	2.594
C30 – H30···C23	2.850	C30 – H30···C23	2.850
C31···H1 – C1	2.715	C31···H1 – C1	2.734
C32···H1 – C1	2.662	C32···H1 – C1	2.832
C32···H76 – C76	2.867		
C33 – H33···C46	2.826	C33 – H33···C46	2.870
C36 – H36···C64	2.665	C36 – H36···C64	2.789
C37···H54 – C54	2.731	C37···H54 – C54	2.864
C54 – H54···C37	2.731	C54 – H54···C37	2.864
C55···H78 – C78	2.822		
C62 – H62···C72	2.815	C62 – H62···F2	2.581
C62 – H62···F2	2.583	C63···H11 – C11	2.794
C63···H11 – C11	2.730		
C63 – H63···Cl 1	2.936		
C64 – H64···Cl 2	2.936	C64···H36 – C36	2.788
C64···H36 – C36	2.665		
C70 – H70···C14	2.847		
C72···H62 – C62	2.815		
C76 – H76···C32	2.867		
C78 – H78···C55	2.822		

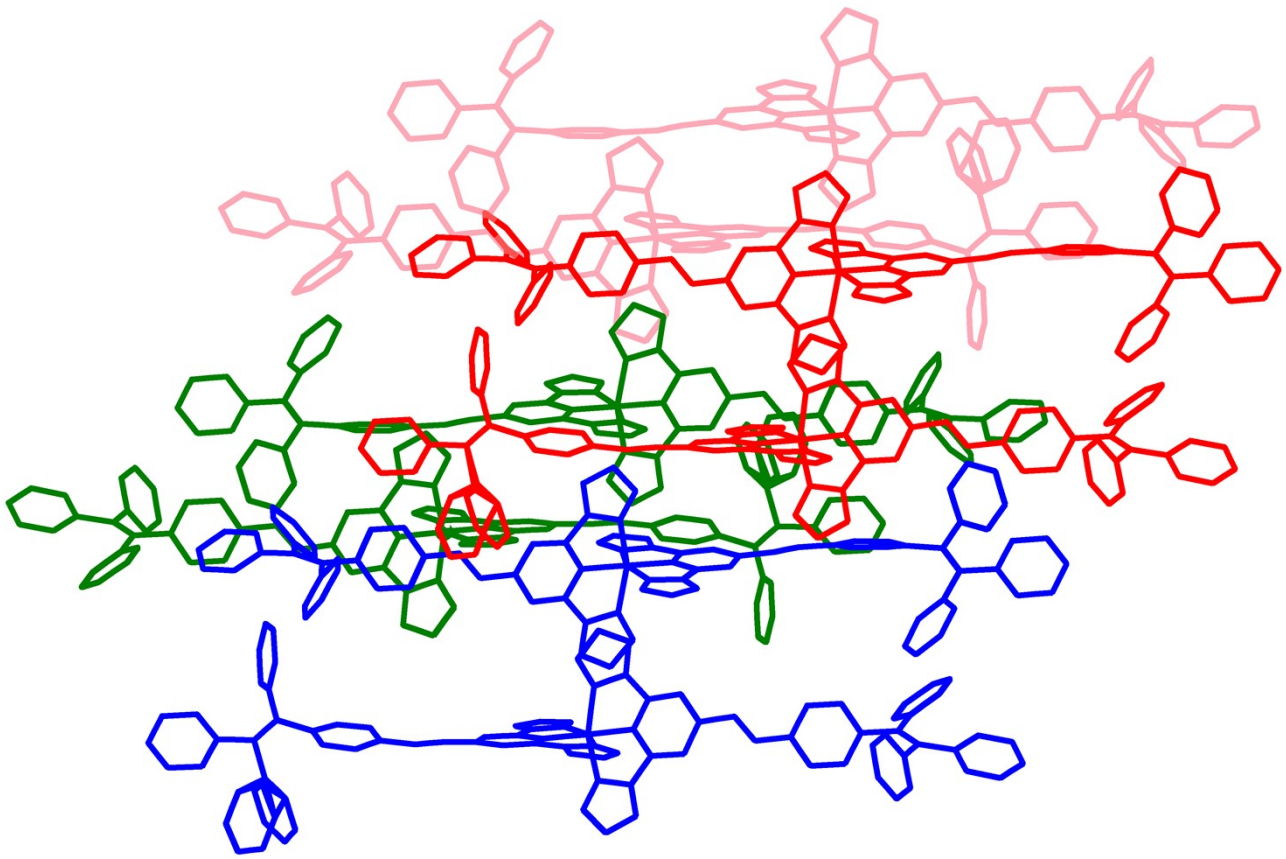

Fig. S25 Crystal packing diagram of complex **1**.

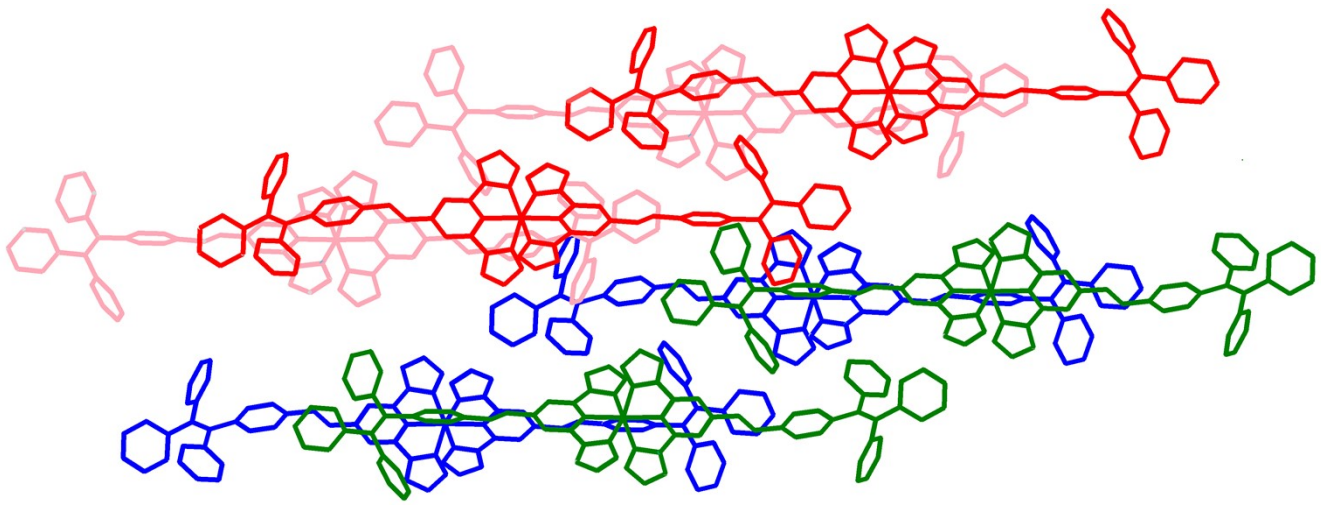

Fig. S26 Crystal packing diagram of complex **2**.

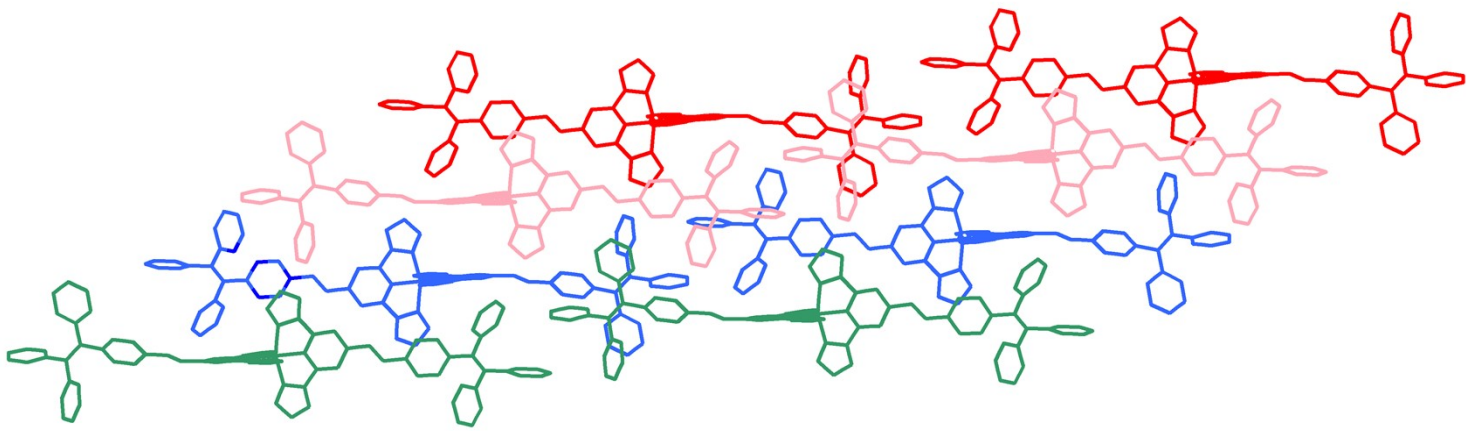

Fig. S27. Crystal packing diagram of complex **3**.